Visual Neuroscience (2006), **23**, 247–256. Printed in the USA.

DOI: 10.1017/S0952523806232097

Sensitivity to visual motion in amblyopic macaque monkeys

LYNNE KIORPES, CHAO TANG, AND J. ANTHONY MOVSHON
Center for Neural Science, New York University, New York, New York

(RECEIVED October 20, 2005; ACCEPTED January 2, 2006)

Abstract

Amblyopia is usually considered to be a deficit in spatial vision. But there is evidence that amblyopes may also suffer specific deficits in motion sensitivity as opposed to losses that can be explained by the known deficits in spatial vision. We measured sensitivity to visual motion in random dot displays for strabismic and anisometropic amblyopic monkeys. We used a wide range of spatial and temporal offsets and compared the performance of the fellow and amblyopic eye for each monkey. The amblyopes were severely impaired at detecting motion at fine spatial and long temporal offsets, corresponding to fine spatial scale and slow speeds. This impairment was also evident for the untreated fellow eyes of strabismic but not anisometropic amblyopes. Motion sensitivity functions for amblyopic eyes were shifted toward large spatial scales for amblyopic compared to fellow eyes, to a degree that was correlated with the shift in scale of the spatial contrast sensitivity function. Amblyopic losses in motion sensitivity, however, were not correlated with losses in spatial contrast sensitivity. This, combined with the specific impairment for detecting long temporal offsets, reveals a deficit in spatiotemporal integration in amblyopia which cannot be explained by the lower spatial resolution of amblyopic vision.

Keywords: Amblyopia, Visual motion sensitivity, Contrast sensitivity, Temporal integration

Introduction

Amblyopia is typically considered to be a disorder of spatial vision. Amblyopia is typically defined by a loss of visual acuity of at least a factor of two in grating acuity, or two lines on a letter chart. However, this definition is only loosely held as the relationships between letter chart performance and other forms of acuity are not consistent or uniformly correlated (see e.g. McKee et al., 2003). Recent work has shown a much broader range of deficits in amblyopes that are not easily explained by or correlated with the basic loss in spatial vision. For example, contour integration and other tasks that require spatial integration are impaired in amblyopia (Hess et al., 1997; Hess & Demanins,1998; Kovács et al., 2000; Mussap & Levi, 2000; Chandna et al., 2001; Kozma & Kiorpes, 2003). Such "high-level" abilities as the perception of illusions (Popple & Levi, 2000) and individuation of features within an image (Sharma et al., 2000) are reportedly abnormal in amblyopes. Although low-level orientation discrimination is largely found to be normal in amblyopes (e.g. Mussap & Levi, 1999; Hess & Malin, 2003; but see Skottun et al., 1986), global orientation detection, particularly in the presence of added noise, is impaired (Simmers & Bex, 2004; Simmers et al., 2005; but see also, Liu et al., 2004).

Many studies have addressed the question of whether amblyopes also suffer losses in temporal vision (see Asper et al., 2000, for review). Monkeys with a history of monocular deprivation show losses of sensitivity to temporal modulation of a uniform field across the temporal-frequency range (Harwerth et al., 1983). Impaired detection of low temporal, high spatial-frequency drifting or oscillating grating targets is often reported (Hess et al., 1978; Manny & Levi, 1982; Bradley & Freeman, 1985; Hess & Anderson, 1993; Ellemberg et al., 2000), and dynamic displacement thresholds are elevated in amblyopes (Buckingham et al., 1991; Kelly & Buckingham, 1998). Some but probably not all of these deficits may be explained by altered spatial vision of the amblyopic visual system (Levi et al., 1984; Steinman et al., 1988; Chung & Levi, 1997).

It remains uncertain whether these losses in spatial and temporal vision predict a greater disorder of motion perception in amblyopia. Hess and Anderson (1993) measured contrast threshold for discrimination of direction of motion over a range of spatial and temporal frequencies. Over most of the range, amblyopes could discriminate motion direction at contrast threshold; they concluded that there is no primary motion deficit. Kubova et al. (1996) reached similar conclusions from motion-onset visual-evoked potential (VEP) measurements. On the other hand, Hess et al. (1997) found that motion aftereffect duration was reduced and took this to indicate a specific deficit in motion processing in amblyopes. Finally, Giaschi et al. (1992) and Simmers et al. (2003) used second-order (contrast defined) motion tasks and found deficits in motion processing that could not easily be related to first-order (luminance-based) losses. These losses are larger than correlated losses in global form discrimination, at least for the specific spatial and temporal conditions used (Simmers et al.,

Address correspondence and reprint requests to: Lynne Kiorpes, Center for Neural Science, 4 Washington Place, Room 809, New York, NY 10003, USA. E-mail: lynne@cns.nyu.edu

2005). These studies concluded that the deficits in second-order motion perception were based in the motion pathway and were likely to be due to mechanisms downstream of primary visual cortex.

We have investigated the extent and nature of losses in motion processing in a nonhuman primate model of amblyopia. We used random-dot kinematograms to assess sensitivity to direction of motion in experimentally amblyopic monkeys. Unlike any previous study, we used a wide range of spatial and temporal parameters for the kinematograms in order to study the full range of motion sensitivity. It is important to study the psychophysical characteristics of amblyopia in monkeys because a wide range of stimulus conditions can be assessed within an individual subject and the underlying neural deficits can be studied directly. Previous work in monkeys suggests that sensitivity to coherent motion in extended random-dot patterns depends on the function of areas such as MT/V5 and MST, downstream of the primary visual cortex (Newsome & Pare, 1988; Britten et al., 1992; Celebrini & Newsome, 1995). Our data reveal substantial deficits in motion processing in amblyopia, which depend on the underlying spatial and temporal parameters of the stimulus and affect the fellow eyes of strabismic amblyopes as well as amblyopic eyes of strabismic and anisometropic amblyopes. While part of this deficit reflects the changes in spatial scale that are characteristic of amblyopic vision, there are additional deficits in the integration of motion signals that suggest a specific effect of amblyopia on downstream processing of motion information.

Some of these data were presented in the doctoral dissertation of C. Tang (Tang, 1999).

Materials and methods

Subjects

Subjects in this study were nine amblyopic *Macaca nemestrina* monkeys, ranging in age at the time of testing from 14 months to 3 years (see Table 1). Comparison data from nine visually normal controls were taken from similarly aged animals tested as part of a study of normal development (Kiorpes & Movshon, 2004). All animals were born at the Washington National Primate Research Center, and were hand-reared in the Visual Neuroscience Laboratory at New York University. All animal care and testing was approved by the New York University UAWC, and conformed to the NIH *Guide for Care and Use of Laboratory Animals*. The visual environment was a normal laboratory environment, which was enriched with a wide variety of appropriate visual and tactile stimuli. The animals were also given daily opportunities for interaction with other monkeys and humans.

Amblyopia developed following either induced strabismus in infancy or rearing with optical defocus. Spatial resolution, measured near the age of motion sensitivity testing by extrapolating the high-frequency fall-off of the contrast sensitivity function to 1 (see below), is listed in Table 1. We do not use an explicit quantitative criterion for determining whether or not an animal is an amblyope. Instead, we use data collected over a variety of measures of spatial vision such as vernier acuity (Kiorpes, 1992; Kiorpes et al., 1993) and contrast sensitivity across the full range of spatial vision (e.g. "amblyopia index", Kiorpes et al., 1998; Kozma & Kiorpes, 2003) to establish a consistent and reliable difference between the eyes. The amblyopia index, computed by taking the area between the fitted contrast sensitivity functions for each eye and dividing it by the area under the function for the fellow eye, is smaller than 0.15 for normal animals. All animals in this study had an amblyopia index of greater than 0.24. Recent contrast sensitivity data from most of the animals in this study have been published (Kozma & Kiorpes, 2003, Figs. 5 and 6).

Experimental strabismus was induced in four monkeys 25–31 days after birth (see Kiorpes, 1992; Kiorpes et al., 1993; Kiorpes & Wallman, 1995). Esotropia (inward deviation) of the left eye was created by transection of the left lateral rectus muscle; the left medial rectus muscle was resected and advanced to the limbus and the conjunctiva was reattached to the globe. Surgery was carried out under ketamine hydrochloride sedation using sterile surgical techniques. The resulting esotropia was moderate, ranging from 10 to 25 prism diopters. The angle of deviation was estimated by the Hirschberg method from photographs; these estimations are accurate to about 5 prism diopters (see Kiorpes et al., 1989, for details). One of the strabismic animals developed an alternating fixation pattern (WW; see Table 1); the others used the nondeviated eye preferentially.

Anisometropia was simulated in five monkeys by inserting a −10 D extended-wear soft contact lens in the right eye and a zero-power lens in the left (see Kiorpes et al., 1993) 20–25 days after birth. The monkeys wore the lenses continuously for a period of up to 8 months. The status and condition of the lenses were checked at 4-h intervals throughout each day. Episodes of missing

Table 1. *Information on the amblyopic monkey subjects*

				Extrapolated acuity (cycles/deg)		Refractive errors	
Monkey	Condition	Onset age (days)	Age at test (year)	Fellow eye	Amblyopic eye	Fellow eye	Amblyopic eye
TX	Strab	26	2.5	18.8	5.2	+2.50-0.50 × 180	+6.50-0.25 × 20
WW	Strab	31	3.1	16.8	12.7	+0.25	+0.25
HF	Strab	25	2.2	24.5	7.1	plano-0.50 × 180	plano
HN	Strab	27	1.9	15.5	3.8	−0.50	+4.50-1.00 × 90
CY	Lens	25	1.6	23.4	6.9	+0.25	+8.50-1.00 × 180
CM	Lens	20	1.7	12.2	6.5	plano-0.25 × 180	+7.50-0.50 × 180
HK	Lens	24	1.2	12.6	10.4	+1.00-0.25 × 180	+6.50
IR	Lens	24	1.3	18.4	9.8	+1.50	+5.50
DG	Lens	23	1.3	14.5	6.2	+1.25-0.50 × 180	+2.50-0.50 × 180

lenses were more common during the first 4 weeks of lens wear with plano lenses out more frequently than blurring lenses (see Kiorpes et al., 1993). Beyond this time period, missing lenses were infrequent (0.34 per week on average). In all cases, missing lenses were replaced immediately. The lenses were changed and cleaned weekly. Regular ophthalmic examinations were performed to insure the health of the eyes. Eye alignment was evaluated by inspection daily and by the Hirschberg method once during rearing. No strabismus was obvious during the rearing period or thereafter in any of the lens-reared animals; however, we would not have detected a tropia or phoria of less than 5 prism diopters.

Other behavioral measurements from the animals in this study have been published (Kiorpes et al., 1999; Kozma & Kiorpes, 2003).

Refractive errors were evaluated during rearing in all subjects. For refraction, both eyes were dilated with 1–3 drops of 2.5% phenylephrine hydrochloride and 3 drops of 0.5% or 1% cyclopentolate. Each strabismic monkey was refracted at least twice within the first postnatal year; the lens-reared monkeys were refracted every 1–2 months. All refractions were performed by the same pediatric ophthalmologist. All monkeys had essentially equal refractive errors in the two eyes at the beginning of rearing. Refractive errors measured closest to the age at test are listed in Table 1. Two strabismic monkeys developed natural anisometropia of greater than 2 diopters during the first postnatal year (TX & HN) and thus may be considered compound amblyopes. Four of the lens-reared monkeys developed natural hyperopic anisometropia of greater than 2 diopters (all except DG). Three became anisometropic during the lens-rearing period; one monkey developed anisometropia after the lenses were removed (IR).

Stimuli

Stimuli were presented on a Nanao T660i monitor subtending 16 deg at 100 cm, the typical viewing distance used. For random-dot displays, the background luminance was 0.3 cd/m^2, and the dot luminance was 112 cd/m^2. Dot size was typically 5.25 min of arc and the displays contained a minimum of 32 dots per frame. Three of the amblyopic animals (TX, HF, & HN) benefited from a shorter viewing distance (50 cm), increased dot size (maximum 14 min arc per dot), and/or an increased number of dots (maximum 48 dots/frame) when viewing with the amblyopic eye. For gratings, the mean luminance was 56 cd/m^2. Stimulus presentation was controlled by a PC computer *via* an ATVista graphics board (Truevision, Inc., Indianapolis, IN).

The motion stimuli were random-dot kinematograms, conceptually similar to those devised by Morgan and Ward (1980) but implemented as described by Britten et al. (1992) (see also, Kiorpes & Movshon, 2004). The kinematograms were presented inside a square field in the center of the display; this field subtended between 7.7 and 18.8 deg, depending on viewing distance. Each frame of this stimulus contained a fixed number of dots that changed position from frame to frame. Any given dot at time t appeared at a location (x, y). At time $t + \Delta t$, with a probability that we term the *coherence*, the dot reappeared at location $(x + \Delta x, y)$. The coherence determined the strength of the global motion signal. If the dot did not reappear, it was replaced by a new dot at a random location. The total number of dots was the same on each frame. The number of appearances of any given dot was related to the coherence. For instance, if the coherence was 0.2, the probability of a dot reappearing once was 0.2, twice was 0.04, and three times was 0.008. Because dot lifetime was limited, it was difficult to judge direction by tracking any single dot or a group of dots (except, of course, when the coherence approached 1). The speed of coherent motion was $\Delta x/\Delta t$, while the incoherent dots provided a masking motion background whose speeds and directions were essentially uniform in distribution.

Behavioral methods were similar to those described elsewhere. We used standard operant conditioning techniques to measure coherence thresholds (Kiorpes et al., 1993; Kiorpes & Movshon, 1998). The psychophysical task was a two-alternative forced-choice directional discrimination. A rectangular field of random dots appeared in the center of the display screen; coherent motion was translational, either rightward or leftward. Stimulus duration was 500 ms at minimum, after which time the animal was free to respond. The subject indicated the direction of motion by pulling one of a pair of grab bars located within reach; a squirt of apple juice was delivered following correct responses. Testing was monocular; appropriate optical correction was provided as needed (Kiorpes & Boothe, 1984). The fellow eye was typically tested first so that any beneficial effect of practice was accorded the amblyopic eye.

We measured coherence threshold by varying the strength of the motion signal across trials using the method of constant stimuli. We fit psychometric functions, based on 3–5 coherence levels, and at least 60 trials per level, for each of a range of Δx and Δt values. Data collection was counterbalanced across Δx for a given Δt, and across Δt. Threshold estimates (75% correct) and associated standard errors were calculated using Probit analysis (Finney, 1971) of the log-transformed data sets. We took motion sensitivity as the inverse of coherence at threshold.

To compare motion sensitivity with basic spatial vision, we measured full spatial contrast sensitivity functions. Contrast sensitivity was measured using conventional methods for our lab (Kiorpes et al., 1993). Sinusoidal gratings were generated under computer control with the same video display system as was used for motion testing. Grating patches were vignetted by a two-dimensional spatial Gaussian (standard deviation = 0.75 deg, except for very low spatial frequencies for which the standard deviation was increased to keep at least three grating cycles visible). Spatial frequencies ranged from 0.3 cycle/deg to 16 cycles/deg; viewing distance ranged from 0.5 m to 2 m, depending on spatial frequency and depth of amblyopia. The monkey's task was to detect the presence of the grating patch on either the right or left side of an otherwise homogeneous gray field that matched the grating in space-average luminance. Threshold values and standard errors of estimate were obtained by Probit analysis of the log-transformed data sets (Finney, 1971) using a maximum-likelihood technique.

We used an iterative method to fit a double-exponential function (Wilson & Bergen, 1979; Kiorpes et al., 1993; Kiorpes & Movshon, 2004) to both motion and contrast sensitivity data. To extract the value of peak sensitivity and its location on the abscissa for each data set, we needed to obtain an unbiased fit regardless of the number of data points in each individual data set. To do this, we used a multiple-set fitting procedure (Movshon & Kiorpes, 1988; Kiorpes & Kiper, 1996). All of the data for each group of interest (e.g. amblyopic eye contrast sensitivity functions, control motion sensitivity functions, etc.) were fit simultaneously to compute a common template curve for the multiple-data set. That template curve was then translated in log–log space to locate the peak of the function for each individual data set within the group. The values of peak sensitivity and scale were extracted from the resulting fits.

Results

We measured motion sensitivity for dot displacements ranging from 1.8 min of arc to 85 min of arc for each eye of each amblyopic animal. Data from two strabismic and two anisometropic amblyopes are plotted in Fig. 1. Motion sensitivity (inverse of coherence threshold) is plotted as a function of dot displacement (Δx) for a given value of temporal offset (Δt), which in this case was 19 ms. Open symbols represent fellow eye data and filled symbols represent amblyopic eye data; the fits to the data are double-exponential functions fit individually (see *Methods*). It is clear from Fig. 1 that the actual pattern of loss in amblyopia varies across subjects and displacement. Some animals show similar overall motion sensitivity for each eye, meaning that the height of the fellow and amblyopic eye functions is similar (e.g. panel D), others show a uniform depression of sensitivity to motion so that substantially higher coherence levels are required for direction discrimination with the amblyopic eye compared to the fellow eye (e.g. panels B & C). Interestingly, the deficit is also dependent on displacement. In most cases, sensitivity for the amblyopic eye is *higher* than for the fellow eye at large Δx but is severely reduced at small Δx.

The corresponding speed values for the $\Delta x/\Delta t$ range plotted in Fig. 1, assuming a 100-cm viewing distance, are shown at the top of the figure. This range includes the fastest speeds we tested. While sensitivity varies little with Δt over the range we used in normal adult monkeys and humans (Baker & Braddick, 1985; Braddick et al., 2003; Alliston, 2004; Kiorpes & Movshon, 2004), some amblyopes showed quite large variation in sensitivity with increasing Δt. Fig. 2 shows raw data for fellow (A, B, E, F) and amblyopic (C, D, G, H) eyes of two monkeys. Data for anisometropic amblyopic monkey IR and strabismic monkey TX are plotted as a function of Δx (right panels) and speed (left panels); the different symbols represent different temporal offsets. IR's fellow eye shows the pattern typical of normal adult animals: sensitivity is independent of Δt within the tested range and performance is thus best captured as dependent on dot displacement rather than dot speed. Note that "peak" motion sensitivity appears to shift to slower speeds with longer Δt (Fig. 2A), while the functions are nearly identical when plotted as a function of displacement (Fig. 2B). IR's amblyopic eye shows a trend that is different from normal and from her fellow eye but representative of amblyopic eyes: sensitivity falls with increasing Δt. Data from a strabismic amblyope, TX (Figs. 2E–2H), show that the amblyopic pattern is reflected in *both* the fellow and amblyopic eye for this monkey. Each of these animals is representative of its group, strabismic or anisometropic; fellow eyes of strabismic amblyopes showed the abnormal, amblyopic pattern of impaired sensitivity with increasing temporal offset whereas fellow eyes of anisometropic amblyopes were similar to controls. Thus, due to the fellow eye abnormality in strabismics, the interocular deficit for strabismic amblyopes was similar across Δt, whereas the deficit grew with Δt for anisometropic amblyopes.

The decline in motion sensitivity with long Δt suggests that there is a particular temporal integration deficit in amblyopia that is more severe in strabismic than anisometropic amblyopia. To evaluate the nature of the temporal processing loss, we measured the slope of the motion sensitivity versus Δt functions across the range of Δx values tested for all groups using this equation:

$$\log(S) = s_0 + k\Delta t, \tag{1}$$

where S is sensitivity, s_0 is the extrapolated sensitivity for $\Delta t = 0$, and Δt is temporal offset. Figs. 3A and 3B illustrate these functions

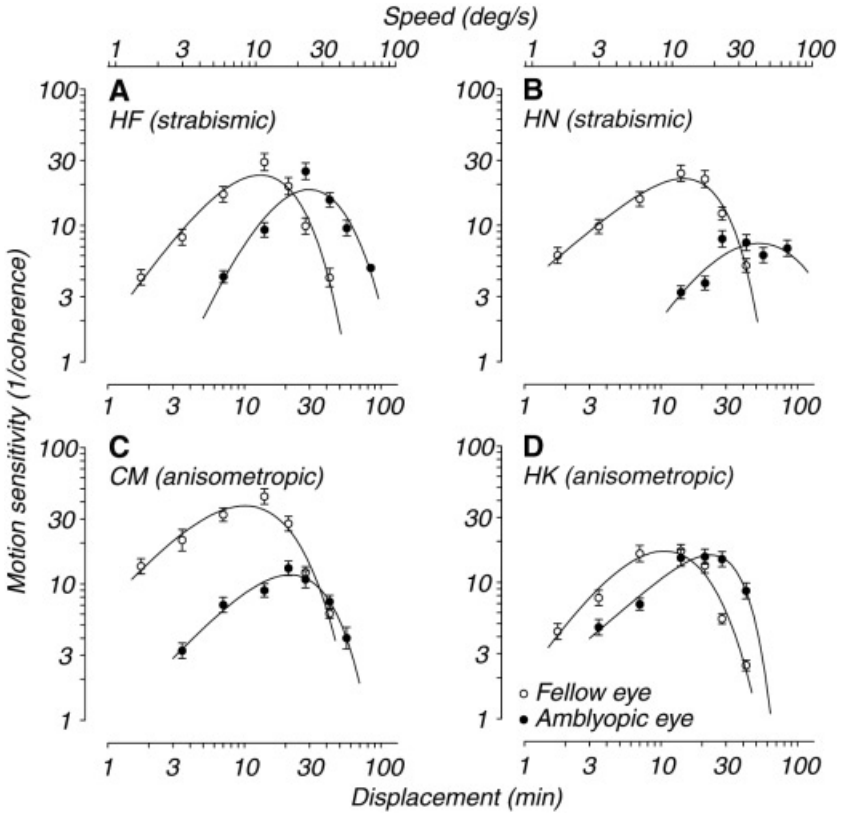

Fig. 1. Motion sensitivity in four amblyopic monkeys. Each panel plots the inverse of the coherence of a random-dot kinematogram stimulus at threshold against the dot displacement (Δx, lower abscissas) and the speed of coherent motion (100-cm viewing distance; upper abscissas), for the two eyes of an amblyopic macaque monkey. Open symbols show data from the untreated fellow eyes, filled symbols from the treated amblyopic eyes. A, B: Data from two strabismic amblyopes. C, D: Data from two anisometropic amblyopes. Δt was 19 ms in all cases.

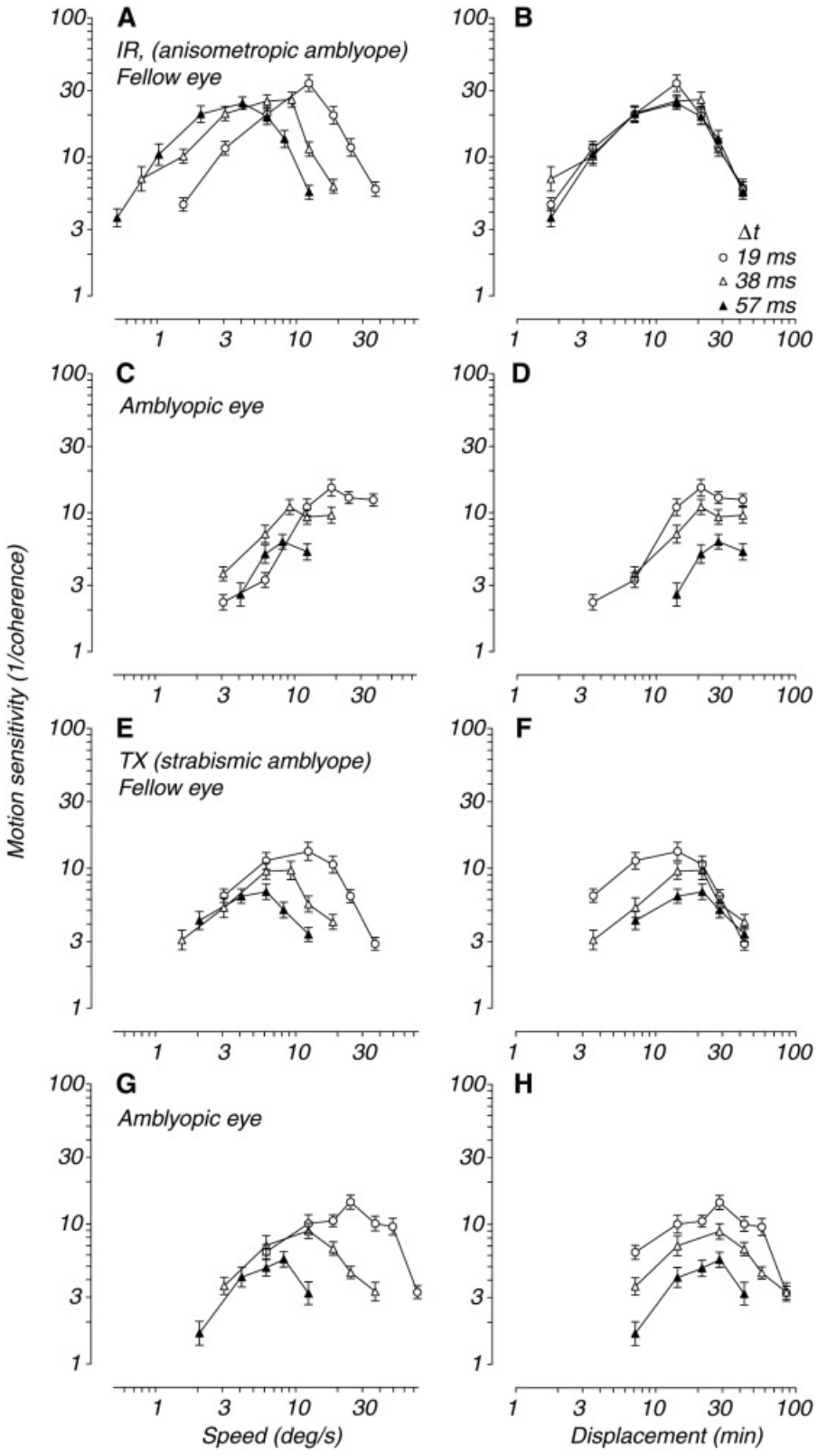

Fig. 2. Spatio-temporal influences on motion sensitivity in two amblyopic monkeys. Each left–right pair of panels plots the same data for one eye of an amblyopic monkey, measured at Δt values of 19, 38, and 57 ms. The left panels (A, C, E, G) plot the data as a function of the speed of coherent motion ($\Delta x/\Delta t$). The right panels (B, D, F, H) plot the same data as a function of the spatial displacement of the dots (Δx). A, B: Data from the fellow eye of an anisometropic amblyope. C, D: Data from the amblyopic eye of the same anisometropic amblyope. E, F: Data from the fellow eye of a strabismic amblyope. G, H: Data from the amblyopic eye of the same strabismic amblyope.

for two displacement values from monkey IR (data taken from Figs. 2B & 2D). Amblyopic eye slopes are clearly steeper than fellow eye slopes in these examples. As there was no significant correlation of the slope k with Δx, we pooled across Δx for the analysis (amblyopic eyes: $F = 0.201$, df 1,33, $P = 0.66$; fellow eyes: $F = 2.83$, df 1,45, $P = 0.1$). The distribution of k is shown for each subgroup in Figs. 3C–3G. There are fewer observations for the strabismic amblyopes because there were fewer strabismic

subjects, their range of Δx sensitivity was smaller in general than the anisometropic amblyopes, and one animal, HN, could not perform the task at the longest Δt using either eye. The white arrows indicate the mean slope for each distribution. For negative values of k, eqn. (1) fits a negative exponential function, and the mean value of $(-1/k)$ can be taken as a measure of the integration time for the motion system. This mean integration time for each group is plotted in Fig. 3H. It is clear that amblyopes have a disorder of temporal integration: their integration time is substantially reduced from normal. Moreover, strabismic amblyopes have this deficit in their fellow eyes as well as their amblyopic eyes.

Sensitivity to motion in random-dot displays depends on both spatial and temporal displacement. As noted above, we found amblyopic eye motion sensitivity functions to be shifted to larger ranges of dot displacement relative to fellow eyes. If the shift in Δx range in amblyopia is due to reduced overall spatial contrast sensitivity, we should expect to find a parallel between an animals' ability to resolve spatial detail and discriminate motion. To explore this relationship, we used motion sensitivity and contrast sensitivity data collected from individual animals at comparable ages and evaluated the spatial scale and sensitivity parameters of both functions. There is no absolute basis for comparison between the spatial-frequency dependence of contrast sensitivity and the spatial offset dependence of motion sensitivity. For grating detection, it is reasonable to assume that mechanisms tuned to the test frequency are responsible for detection. But the directional information in a random-dot display is present at a wide range of spatial frequencies, and can in principle be analyzed by mechanisms sensitive to any informative spatial frequency. Smith et al. (2002) studied the responses of real and simulated neurons in V1 and MT to dynamic Glass patterns, which are analogous to our random-dot kinematograms except that the underlying Δt is 0. They concluded that neuronal responses were most informative when Δx corresponded to roughly half the wavelength of the optimal spatial frequency; this also corresponds to the first point of maximal anisotropy in the spatial-frequency spectrum of a static dot pattern. For comparison purposes, we therefore take $1/2\Delta x$ as the "equivalent spatial frequency" of a kinematogram, as in Kiorpes and Movshon (2004).

Fig. 4 shows example data from two monkey amblyopes, one strabismic (A & C) and one anisometropic (B & D). In the top panels, we show standard contrast sensitivity data for each eye of each animal. In the bottom panels, we plot motion sensitivity as a function of "equivalent" spatial frequency on an aligned axis. It appears from these examples that shifts in spatial scale are similar for motion and contrast sensitivity, while there is no consistent parallel shift in overall sensitivity (the height of the curves). TX and CM show a shift to larger spatial scale with the amblyopic eye for both motion and contrast sensitivity. TX shows reduced sensitivity to contrast with the amblyopic eye compared to the fellow eye but no difference in overall coherence sensitivity. CM has

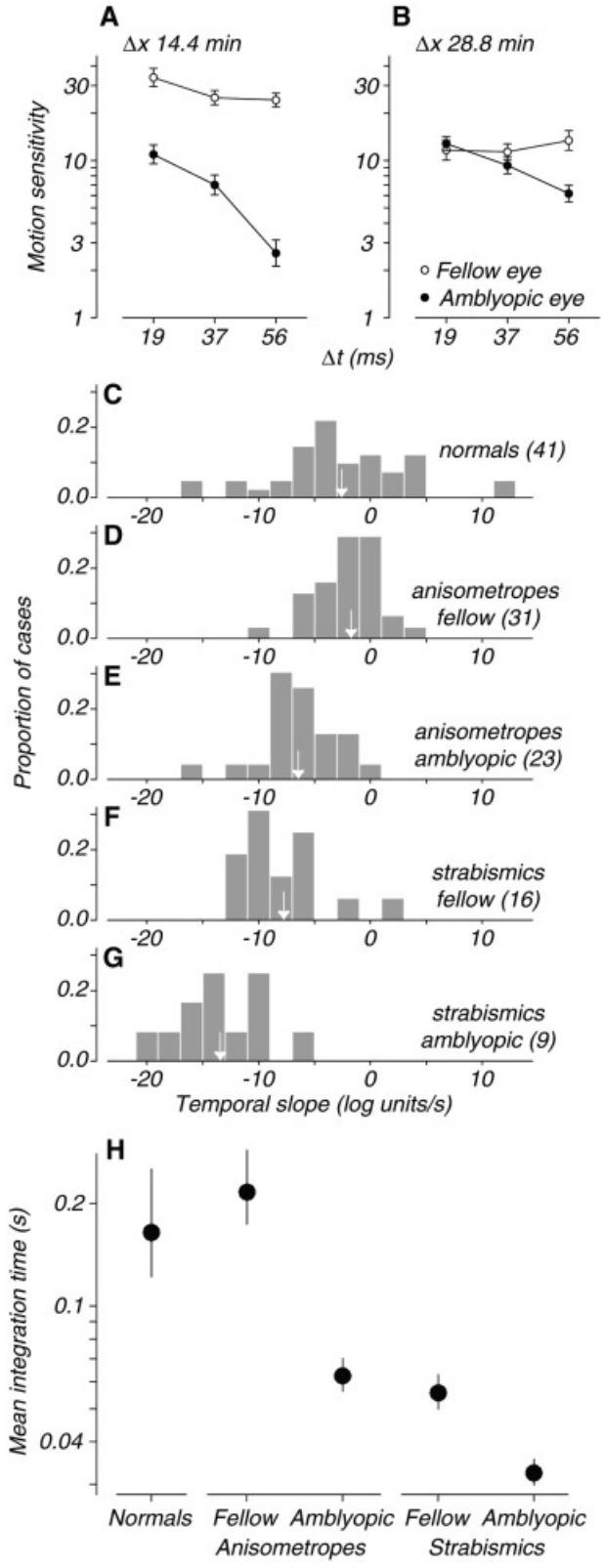

Fig. 3. Analysis of temporal integration in motion detection. A, B: Motion sensitivity as a function of Δt for an anisometropic amblyope at two values of Δx (14.4 & 28.8 min). Open symbols show data from the untreated fellow eye, filled symbols from the treated amblyopic eye. Temporal sensitivity functions like these were described with the simple exponential function given in the text as equation (1). C–G: Distributions of the slopes of the temporal integration functions for five test conditions: normal eyes (C), fellow eyes of anisometropic amblyopes (D), amblyopic eyes of anisometropic amblyopes (E), fellow eyes of strabismic amblyopes (F), and amblyopic eyes of strabismic amblyopes (G). H: The average integration time for the five conditions represented in C–G. The symbols represent the inverse of the mean slope for each condition, and the error bars represent the inverses of the mean ± one SE.

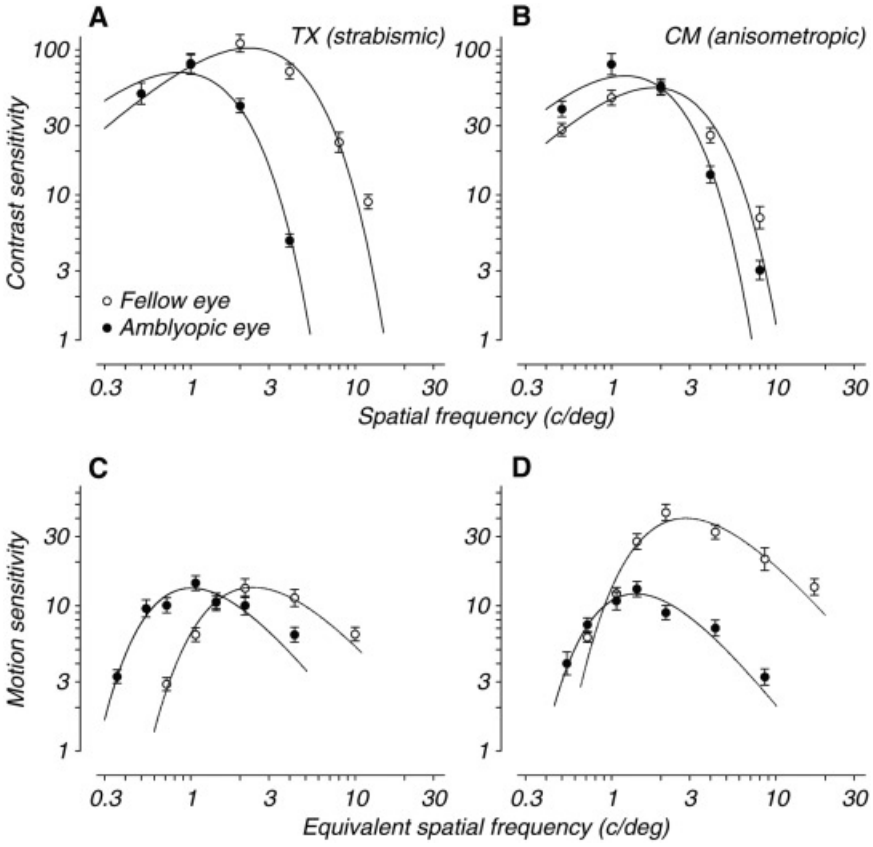

Fig. 4. Comparison of the interocular differences in spatial contrast sensitivity and motion sensitivity for two amblyopes. A, B: Spatial contrast sensitivity functions for the two eyes of a strabismic and an anisometropic amblyope. C, D: Motion sensitivity functions for the two eyes of the same two monkeys. The motion sensitivity functions are plotted against "equivalent spatial frequency" ($1/2\Delta x$, see text for details) to facilitate comparison. Open symbols show data from the untreated fellow eyes, filled symbols from the treated amblyopic eyes.

higher peak contrast sensitivity with the amblyopic eye but substantially poorer motion sensitivity with that eye. To see whether these animals are representative of the population, we collected the contrast sensitivity and motion sensitivity functions for each group and data type (e.g. fellow eyes' motion sensitivity, control eyes' contrast sensitivity; see Methods). For this analysis, we used only data from 19-ms Δt conditions as these conditions uniformly resulted in the best performance from the amblyopes. We computed the appropriate shape parameters for each set of data. We used those shape parameters to define a template curve for each group and data type, which was then fit to each individual data set. From the resulting fits, we extracted the location of the peak in sensitivity and scale: peak motion and spatial contrast sensitivity, and best displacement and spatial frequency.

Figs. 5A and 5B show an interocular comparison of spatial scale and sensitivity for motion and contrast sensitivity data for each monkey. The lines in each panel connect the data for the two eyes of each monkey, open symbols for the fellow eyes, and filled symbols for the amblyopic eyes. Each monkey's data are represented by the same color in the two panels; reddish points are for anisometropes, bluish for strabismics. Plusses show data for age-matched control animals. Comparison of the two panels reveals a more consistent relationship between measures of scale (A) than between measures of sensitivity (B). Taking all eyes together, the correlation between peak displacement and peak spatial frequency is significant ($r = 0.79$, $n = 27$, $P < 0.00001$) while that for motion and contrast sensitivity is not ($r = 0.34$, $n = 27$, $P = 0.08$). This difference is reflected in the relationship between measures of scale and sensitivity in the amblyopic and fellow eyes (lines; the insets at the top left of each plot center all the lines connecting data for the two eyes of amblyopes). In most cases, there appears to be a systematic relationship between the shift in spatial scale of the contrast sensitivity function and that of the motion sensitivity function (Fig. 5A); eight of nine animals show a shift to larger spatial scale for both motion and contrast sensitivity with the amblyopic eye compared to the fellow eye. There is more scatter in the sensitivity data (Fig. 5B); only four of the nine animals show shifts that are roughly proportional, suggesting that there is a weaker relationship between motion sensitivity and contrast sensitivity than for spatial displacement and frequency. It is not possible to tell whether this difference is specifically related to the amblyopic changes—note, for example, that the normal data for scale are much more tightly clustered in Fig. 5A than they are for sensitivity in Fig. 5B. It seems reasonable to conclude that the neural mechanisms determining the spatial scale of both contrast and motion processing are linked, while those determining contrast and motion sensitivity are to some degree independent. This is consistent with a two-stage model, to which we return below.

Discussion

Our data show clear, specific losses in sensitivity to visual motion in amblyopia. The degree of loss depends on dot displacement: for large displacements many amblyopes performed *better* with the amblyopic eye than with the fellow eye, but for small displacements, amblyopic eye performance was consistently compromised. In some cases, coherence sensitivity was similar for the two eyes of an animal at the peak of the motion sensitivity function, although the peak was displaced to larger spatial scales for the amblyopic eye. For the fastest speeds, that is, for large displace-

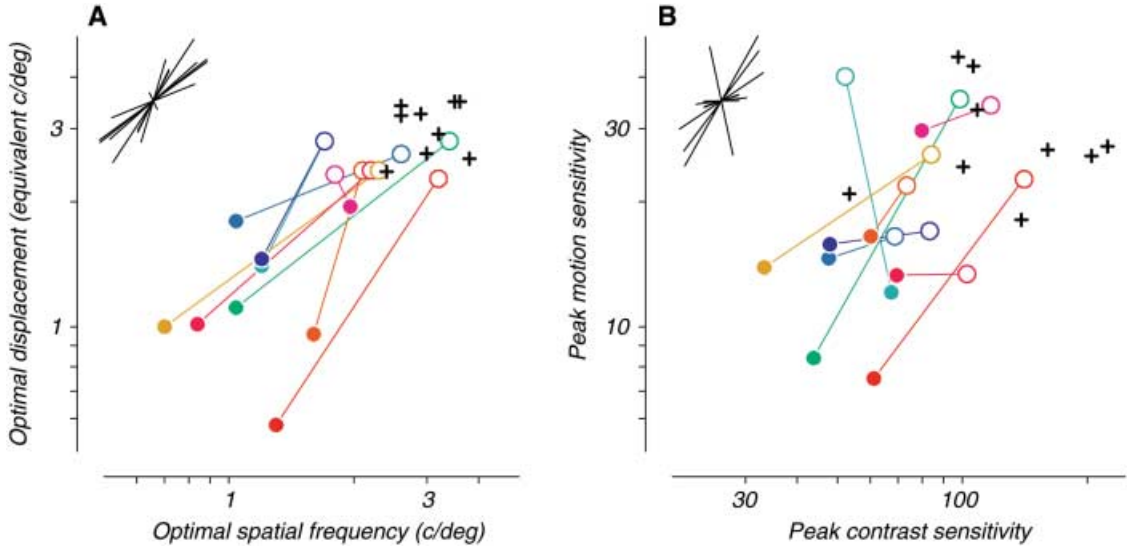

Fig. 5. Interocular comparison of spatial contrast sensitivity and motion sensitivity for all amblyopic animals. A: The spatial scale of visual performance is represented by the optimal spatial frequency from the spatial contrast sensitivity function (abscissa), and the spatial scale of motion sensitivity is represented by the optimal Δx, plotted as "equivalent spatial frequency" (ordinate; see Fig. 4). B: The sensitivity of visual performance is represented by the peak contrast sensitivity in the spatial domain (abscissa), and the sensitivity for motion discrimination is represented by the peak motion sensitivity (ordinate). Filled symbols represent data from the amblyopic eyes, open symbols represent data from the fellow eyes, and lines connect the data for the two eyes of each animal. The plusses show the comparisons for the control monkeys. Inset into the top left of both panels, at half scale, are centered copies of the lines connecting the two data points for each animal in the respective panel.

ments independently of temporal offset, there was no consistent difference between the pattern of loss in anisometropic amblyopes and strabismic amblyopes. However, for slow speeds (fine displacements), where performance was most compromised in the amblyopes, the interocular difference grew larger with increasing temporal offset for anisometropic but not for strabismic amblyopes. This was because the *fellow* eyes of strabismic amblyopes showed decreased sensitivity to coherent motion with increasing temporal offset that paralleled that of the amblyopic eye. Fellow eyes of anisometropic amblyopes did not show this trend. These findings reveal a deficit in spatiotemporal integration in amblyopic vision.

Steinman et al. (1988) reported amblyopic deficits in discrimination of temporal asynchrony and velocity. As we did, they found little or no impairment at fast speeds but increasingly large deficits at slow speeds. Using grating stimuli, Hess and Anderson (1993) measured contrast sensitivity for direction discrimination as compared to motion detection. They reported a selective elevation of direction discrimination thresholds at slow speeds. Similarly, others have reported losses of sensitivity to the combination of high spatial and low temporal frequency counterphase flicker in some amblyopes (Manny & Levi, 1982; Bradley & Freeman, 1985). However, none of these groups identified these losses as specific to temporal processing.

Some amblyopes showed an overall reduction in sensitivity to coherent motion with their fellow eyes compared to the normal control monkeys. Typical adult monkeys show peak motion sensitivity in the range of 25–50, which is achieved by about 3 years after birth (Kiorpes & Movshon, 2004). Since many of the monkeys in this study were younger than 3 years, we used age-matched controls for comparison. Two anisometropic and one strabismic amblyope performed below the range of the controls with the fellow eye showing deficient performance across the full range dot displacements. Losses in fellow eye motion sensitivity have occasionally been noted in human amblyopes (Giaschi et al., 1992; Ho et al., 2005).

The shift of amblyopic eye motion sensitivity toward large dot displacements is consistent with the well-documented shift of the amblyopic contrast sensitivity function toward larger spatial scales (e.g. Kiorpes, 1996). As Fig. 5A shows, the shift in peak displacement is well correlated with the scale shift in the spatial contrast sensitivity function. This scale shift can presumably be explained by the lower spatial-frequency tuning of neurons in visual cortex of amblyopic monkeys (Kiorpes et al., 1998). However, the reduction in coherence sensitivity seen in most amblyopic eyes, and some fellow eyes, is not easily explained by simple, first-order, contrast-dependent losses. The individual dots in our kinematograms would have been clearly visible to the amblyopic monkeys, and the loss of motion sensitivity is not consistently related to the losses in spatial contrast sensitivity in the same animals (Fig. 5B). This result is consistent with recent studies in human amblyopes showing losses in motion integration at a particular slow speed that could not be accounted for by losses in contrast sensitivity (Simmers et al., 2003; Simmers et al., 2005).

We found a striking and specific loss in the ability of the amblyopic visual system to integrate motion signals over time. We estimated the integration time of the normal visual motion system to be near 200 ms, but the amblyopic system could only integrate between 30 and 60 ms (Fig. 3). In strabismic amblyopes, this deficit in temporal integration was apparent for fellow as well as amblyopic eyes (see Fig. 3H).

A potential explanation for the reduced performance of amblyopes might be a reduction in direction movement selectivity, which could impair performance on our direction discrimination task.

Watanabe et al. (2005) recently reported a loss of neuronal direction selectivity in V1 and V2 of nonamblyopic strabismic monkeys, but we did not observe such a loss in our earlier studies of either V1 or MT (Kiorpes et al., 1998, 1996). In the course of another study, we tested five of the same amblyopic monkeys described here (including 3 strabismics) on a 2-alternative detection version of our task, in which the animals had to indicate which one of two dot fields contained coherent motion (unpublished data). This task does not require that the animals discriminate direction. For these five individuals, the interocular ratios of motion sensitivity were very similar on the two tasks ($r = 0.95$, $n = 5$, $P = 0.013$), suggesting that a deficit in direction discrimination is not responsible for the threshold changes we observed in amblyopes.

It is possible that oculomotor instability contributes to the pattern of deficits we found for strabismic amblyopes. Latent nystagmus and nasal-temporal asymmetries in smooth pursuit and optokinetic nystagmus (OKN) have been reported in non-amblyopic strabismics (e.g. Tychsen & Lisberger, 1986; Kiorpes et al., 1996; Valmaggia et al., 2003). Also, infantile esotropes show asymmetry in horizontal motion detection (Bosworth & Birch, 2005). However, we detected no such abnormalities in our anisometropic amblyopes nor did we note any obvious response bias to nasalward motion in any of our animals. Moreover, no physiological studies have found a directional asymmetry in neuronal populations recorded from V1, V2, or MT in strabismics (Kiorpes et al., 1996, 1998; Watanabe et al., 2005), suggesting that any asymmetry is not a result of abnormality in the early motion pathways.

It is commonly thought that temporal integration in random-motion displays depends on two factors—the temporal properties of early local motion detectors, and the properties of a later, central pooling mechanism (e.g. Fredricksen et al.,1994*a*,*b*; Morrone et al., 1995). In amblyopes, we argued above that the lower spatial scale of motion detection reflects abnormalities in the spatial scale of local motion detectors, perhaps directionally selective neurons in V1 (Kiorpes et al., 1998). But it is difficult to interpret the reduction in sensitivity at long Δt in this way, since the argument would have to be that local detectors in amblyopes for some reason have far *greater* temporal precision than in normals. It seems much more reasonable to suppose that the defect in temporal integration in amblyopes is due to a breakdown in performance at the second, pooling stage, where signals from many local motion detectors are combined. This idea is also consistent with our observation of temporal integration deficits in the *fellow* eyes of our strabismic amblyopes (Fig. 3). If these non-binocular amblyopes have visual deficits downstream of the basic mechanisms responsible for contrast detection, this fellow-eye deficit can be understood as a change in second-stage mechanisms that receive input from both eyes (see McKee et al., 2003, for a discussion of second-stage deficits in non-binocular amblyopes).

While the deficits related to spatial scale can at least in part be ascribed to reduced spatial scale of the neurons driven by the amblyopic eye in primary visual cortex, the reduction in coherence sensitivity and integration time cannot. Kiorpes et al. (1998) found that, unlike neuronal spatial-frequency tuning, contrast sensitivity for neurons driven by the amblyopic eye in V1 appeared to be unrelated to the deficit in behavioral contrast sensitivity. Temporal tuning and temporal resolution of cortical neurons driven by the amblyopic eye in V1 were also not different from those properties of neurons driven by the fellow eye, reinforcing the view that the inputs to downstream visual mechanisms in amblyopes are largely normal except for their reduced spatial scale. We and others have proposed that the amblyopic visual system has higher levels of internal noise, which would limit the effectiveness of second-stage pooling mechanisms (Wang et al., 1998; Kiorpes et al., 1999; Sharma et al., 2000; Levi & Klein, 2003; Pelli et al., 2004; Simmers et al., 2003, 2005). The reduced integration time that we observed in amblyopes might represent the visual system's way to minimize the impact of this increased noise. Thus, we suggest that the deficits in motion sensitivity in amblyopic monkeys are due to disruption of mechanisms downstream from early motion detectors, presumably in the motion-sensing areas of the extrastriate visual cortex.

Acknowledgments

This work was supported by NIH grants EY05864 to L. Kiorpes and EY02017 to J.A. Movshon, and RR00166 to the Washington National Primate Research Center. Additional support was provided by an investigatorship to J.A. Movshon from the Howard Hughes Medical Institute. We thank Dr. Howard Eggers for clinical care, strabismus surgery, and refractions. We are grateful to Michael Gorman and Jeanine DiMitri D'Agostino for assistance with animal care and testing.

References

Alliston, E.L. (2004). *Glass patterns and random dot motion: Parallel and hierarchical visual processing*. PhD Dissertation, New York University. http://wwwlib.umi.com/dissertations/fullcit/3127423.

Asper, L., Crewther, D. & Crewther, S.G. (2000). Strabismic amblyopia. Part 1: Psychophysics. *Clinical and Experimental Optometry* **83**, 49–58.

Baker, C.L. & Braddick, O. (1985). Temporal properties of the short-range process in apparent motion. *Perception* **14**, 181–192.

Bosworth, R.G. & Birch, E.E. (2005). Motion detection in normal infants and young patients with infantile esotropia. *Vision Research* **45**, 1557–1567.

Braddick, O., Atkinson, J. & Wattam-Bell, J. (2003). Normal and anomalous development of visual motion processing: Motion coherence and 'dorsal-stream vulnerability'. *Neuropsychologia* **41**, 1769–1784.

Bradley, A. & Freeman, R.D. (1985). Temporal sensitivity in amblyopia: An explanation of conflicting reports. *Vision Research* **25**, 39–46.

Britten, K.H., Shadlen, M.N., Newsome, W.T. & Movshon, J.A. (1992). The analysis of visual motion: A comparison of neuronal and psychophysical performance. *Journal of Neuroscience* **12**, 4745–4765.

Buckingham, T., Watkins, R., Bansal, P. & Bamford, K. (1991). Hyperacuity thresholds for oscillatory movement are abnormal in strabismic and anisometropic amblyopes. *Optometry and Vision Science* **68**, 351–356.

Celebrini, S. & Newsome, W.T. (1995). Microstimulation of extrastriate area MST influences performance on a direction discrimination task. *Journal of Neurophysiology* **73**, 437–448.

Chandna, A., Pennefather, P.M., Kovács, I. & Norcia, A.M. (2001). Contour integration deficits in anisometropic amblyopia. *Investigative Ophthalmology and Visual Science* **42**, 875–878.

Chung, S.T. & Levi, D.M. (1997). Moving vernier in amblyopic and peripheral vision: greater tolerance to motion blur. *Vision Research* **37**, 2527–2533.

Ellemberg, D., Lewis, T.L., Maurer, D. & Brent, H.P. (2000). Influence of monocular deprivation during infancy on the later development of spatial and temporal vision. *Vision Research* **40**, 3283–3295.

Finney, D.J. (1971). *Probit Analysis*. New York: Cambridge University Press.

Fredricksen, R.E., Verstraten, F.A.J. & van de Grind, W.A. (1994*a*). An analysis of the temporal integration mechanism in human motion perception. *Vision Research* **34**, 3153–3170.

Fredricksen, R.E., Verstraten, F.A.J. & van de Grind, W.A. (1994*b*). Spatial summation and its interaction with the temporal integration mechanism in human motion perception. *Vision Research* **34**, 3171–3188.

Giaschi, D.E., Regan, D., Kraft, S.P. & Hong, X-H. (1992). Defective processing of motion-defined form in the fellow eye of patients with unilateral amblyopia. *Investigative Ophthalmology and Visual Science* **33**, 2483–2489.

Harwerth, R.S., Smith, E.L. III, Boltz, R.L., Crawford, M.L.J. & von Noorden, G.K. (1983). Behavioral studies on the effects of abnormal early visual experience in monkeys: Temporal modulation sensitivity. *Vision Research* **23**, 1511–1517.

Hess, R.F. & Anderson, S.J. (1993). Motion sensitivity and spatial undersampling in amblyopia. *Vision Research* **33**, 881–896.

Hess, R.F. & Demanins, R. (1998). Contour integration in anisometropic amblyopia. *Vision Research* **38**, 889–894.

Hess, R.F., Demanins, R. & Bex, P.J. (1997). A reduced motion aftereffect in strabismic amblyopia. *Vision Research* **37**, 1303–1311.

Hess, R.F., Howell, E.R. & Kitchin, J.E. (1978). On the relationship between pattern and movement perception in strabismic amblyopia. *Vision Research* **18**, 375–377.

Hess, R.F. & Malin, S.A. (2003). Threshold vision in amblyopia: Orientation and phase. *Investigative Ophthalmology and Visual Science* **44**, 4762–4771.

Hess, R.F., McIlhagga, W. & Field, D.J. (1997). Contour integration in strabismic amblyopia: The sufficiency of an explanation based on positional uncertainty. *Vision Research* **37**, 3145–3161.

Ho, C.S., Giaschi, D.E., Boden, C., Dougherty, R., Cline, R. & Lyons, C. (2005). Deficient motion perception in the fellow eye of amblyopic children. *Vision Research* **45**, 1615–1627.

Kelly, S.L. & Buckingham, T.J. (1998). Movement hyperacuity in childhood amblyopia. *British Journal of Ophthalmology* **82**, 991–995.

Kiorpes, L. (1992). Effect of strabismus on the development of vernier acuity and grating acuity in monkeys. *Visual Neuroscience* **9**, 253–259.

Kiorpes, L. (1996). Development of contrast sensitivity in normal and amblyopic monkeys. In *Infant Vision*, ed. Vital-Durand, F., Atkinson, J. & Braddick, O., pp. 3–15. Oxford: Oxford University Press.

Kiorpes, L. & Boothe, R.G. (1984). Accommodative range in amblyopic monkeys. *Vision Research* **24**, 1829–1834.

Kiorpes, L., Carlson, M.R. & Alfi, D. (1989). Development of visual acuity in experimentally strabismic monkeys. *Clinical Vision Sciences* **4**, 95–106.

Kiorpes, L. & Kiper, D.C. (1996). Development of contrast sensitivity across the visual field in macaque monkeys (*Macaca nemestrina*). *Vision Research* **36**, 239–247.

Kiorpes, L., Kiper, D.C. & Movshon, J.A. (1993). Contrast sensitivity and vernier acuity in amblyopic monkeys. *Vision Research* **33**, 2301–2311.

Kiorpes, L., Kiper, D.C., O'Keefe, L.P., Cavanaugh, J.R. & Movshon, J.A. (1998). Neuronal correlates of amblyopia in the visual cortex of macaque monkeys with experimental strabismus and anisometropia. *Journal of Neuroscience* **18**, 6411–6424.

Kiorpes, L. & Movshon, J.A. (1998). Peripheral and central factors limiting the development of contrast sensitivity in macaque monkeys. *Vision Research* **38**, 61–70.

Kiorpes, L. & Movshon, J.A. (2004). Development of sensitivity to visual motion in macaque monkeys. *Visual Neuroscience* **21**, 851–859.

Kiorpes, L., Tang, C. & Movshon, J.A. (1999). Factors limiting contrast sensitivity in experimentally amblyopic monkeys. *Vision Research* **39**, 4152–4160.

Kiorpes, L. & Wallman, J. (1995). Does experimentally-induced amblyopia cause hyperopia in monkeys? *Vision Research* **35**, 1289–1297.

Kiorpes, L., Walton, P.J., O'Keefe, L.P., Movshon, J.A. & Lisberger, S.G. (1996). Effects of early onset strabismus on pursuit eye movements and on neuronal responses in area MT of macaque monkeys. *Journal of Neuroscience* **16**, 6537–6553.

Kovács, I., Polat, U., Pennefather, P.M., Chandna, A. & Norcia, A.M. (2000). A new test of contour integration deficits in patients with a history of disrupted binocular experience during visual development. *Vision Research* **40**, 1775–1783.

Kozma, P. & Kiorpes, L. (2003). Contour integration in amblyopic monkeys. *Visual Neuroscience* **20**, 577–588.

Kubova, Z., Kuba, M., Juran, J. & Blakemore, C. (1996). Is the motion system relatively spared in amblyopia? Evidence from cortical evoked responses. *Vision Research* **36**, 181–190.

Levi, D.M. & Klein, S. (2003). Noise provides some new signals about the spatial vision of amblyopes. *Journal of Neuroscience* **23**, 2522–2526.

Levi, D.M., Klein, S. & Aitsebaomo, P. (1984). Detection and discrimination of the direction of motion in central and peripheral vision of normal and amblyopic observers. *Vision Research* **24**, 789–800.

Liu, L., Wang, K., Liao, B., Xu, L. & Han, S. (2004). Perceptual salience of global structures and the crowding effect in amblyopia. *Graefe's Archives of Clinical Experimental Ophthalmology* **242**, 566–570.

Manny, R. & Levi, D.M. (1982). Psychophysical investigations of the temporal modulation sensitivity function in amblyopia: Spatiotemporal interactions. *Investigative Ophthalmology and Visual Science* **22**, 525–534.

McKee, S.P., Levi, D.M. & Movshon, J.A. (2003). The pattern of visual deficits in amblyopia. *Journal of Vision* **3**, 380–405.

Morgan, M.J. & Ward, R. (1980). Conditions for motion flow in dynamic visual noise. *Vision Research* **20**, 431–435

Morrone, M.C., Burr, D.C. & Vaina, L.M. (1995). Two stages of visual processing for radial and circular motion. *Nature* **376**, 507–509.

Movshon, J.A. & Kiorpes, L. (1988). Analysis of the development of spatial contrast sensitivity in monkey and human infants. *Journal of the Optical Society of America A* **5**, 2166–2172.

Mussap, A.J. & Levi, D.M. (1999). Orientation-based texture segmentation in strabismic amblyopia. *Vision Research* **39**, 411–418.

Mussap, A.J. & Levi, D.M. (2000). Amblyopic deficit in detecting a dotted line in noise. *Vision Research* **40**, 3297–3307.

Newsome, W.T. & Pare, E.B. (1988). A selective impairment of motion perception following lesions of the middle temporal visual area (MT). *Journal of Neuroscience* **8**, 2201–2211.

Pelli, D.G., Levi, D.M. & Chung, S.T.L. (2004). Using visual noise to characterize amblyopic letter identification. *Journal of Vision* **4**, 904–920.

Popple, A.V. & Levi, D.M. (2000). Amblyopes see true alignment where normal observers see illusory tilt. *Proceedings of the National Academy of Sciences of the U.S.A.* **97**, 11667–11672.

Sharma, V., Levi, D.M. & Klein, S.A. (2000). Undercounting features and missing features: Evidence for a high-level deficit in strabismic amblyopia. *Nature Neuroscience* **3**, 496–501.

Simmers, A.J. & Bex, P.J. (2004). The representation of global spatial structure in amblyopia. *Vision Research* **44**, 523–533.

Simmers, A.J., Ledgeway, T. & Hess, R.F. (2005). The influences of visibility and anomalous integration processes on the perception of global spatial form versus motion in human amblyopia. *Vision Research* **45**, 449–460.

Simmers, A.J., Ledgeway, T., Hess, R.F. & McGraw, P.V. (2003). Deficits to global motion processing in human amblyopia. *Vision Research* **43**, 729–738.

Skottun, B.C., Bradley, A. & Freeman, R.D. (1986). Orientation discrimination in amblyopia. *Investigative Ophthalmology and Visual Science* **27**, 532–537.

Smith, M.A., Bair, W. & Movshon, J.A. (2002). Signals in macaque striate cortical neurons that support the perception of Glass patterns. *Journal of Neuroscience* **22**, 8334–8345.

Steinman, S.B., Levi, D.M. & McKee, S.P. (1988). Discrimination of time and velocity in the amblyopic visual system. *Clinical Vision Sciences* **2**, 265–276.

Tang, C. (1999). *Apparent motion detection in amblyopic monkeys*. PhD Dissertation. New York University. http://wwwlib.umi.com/dissertations/fullcit/9917087.

Tychsen, L. & Lisberger, S.G. (1986). Maldevelopment of visual motion processing in humans who had strabismus with onset in infancy. *Journal of Neuroscience* **6**, 2495–2508.

Valmaggia, C., Proudlock, F. & Gottlob, I. (2003). Optokinetic nystagmus in strabismus: Are asymmetries related to binocularity? *Investigative Ophthalmology and Visual Science* **44**, 5142–5150.

Wang, H., Levi, D.M. & Klein (1998). Spatial uncertainty and sampling efficiency in amblyopic position acuity. *Vision Research* **38**, 1239–1245.

Watanabe, I., Bi, H., Zhang, B., Sakai, E., Mori, T., Harwerth, R.S., Smith, E.L., III & Chino, Y.M. (2005). Directional bias of neurons in V1 and V2 of strabismic monkeys: Temporal-to-nasal asymmetry? *Investigative Ophthalmology and Visual Science* **46**, 3899–3905.

Wilson, H.R. & Bergen, J.R. (1979). A four mechanism model for threshold spatial vision. *Vision Research* **19**, 19–32.